**ORIGINAL PAPER**

# Different fluorescence emitting copper nanoclusters protected by egg white and double-emission fluorescent probe for fast detection of ethanol

Yanyue Li[1] · Yu He[1] · Yili Ge[1] · Gongwu Song[1] · Jiangang Zhou[2]

## Abstract

Green emitting copper nanoclusters (G-Cu NCs), yellow emitting Cu NCs (Y-Cu NCs), orange emitting Cu NCs (O-Cu NCs) and red emitting Cu NCs (R-Cu NCs) were prepared using chicken egg white as the stabilizer by changing the reaction conditions. This is a green, facile and cheap method to explore different color emitting CuNCs by the same precursor and stabilizers. The G-Cu NCs were employed for the detection of ethanol due to their aggregation induced emission enhancement (AIEE) effect. The fluorescence emission of Cu NCs at 526 nm under the excitation of 444 nm can be effectively enhanced in the presence of ethanol due to AIEE effect, thus realizing the quantitative determination of ethanol content in the range 5–60%. In addition, a visual dual-emission fluorescence probe with the combination of G-Cu NCs and silicon nanoparticles (Si NPs/G-Cu NCs) was designed to evaluate ethanol content conveniently and rapidly. Desirable linear relationship is observed between ratio of fluorescence intensity ($I_{525}/I_{441}$) and ethanol content under the excitation of 383 nm. Visible color transformation of this probe is observed in the ethanol content range 2–20%. Moreover, the ethanol sensing platforms were applied to the detection and evaluation of the alcohol content of liquor, and the recoveries in liquor were in the range 99.7% to 113%, broadening the applications of Cu NCs and providing a sensitive detection method for ethanol.

**Keywords** Copper nanoclusters · Chicken egg white · Ratiometric fluorescent sensor · Ethanol determination

## Introduction

Metal nanoclusters (NCs) have attracted extensive attention due to their excellent properties, such as optical stability, low toxicity and good biocompatibility [1–3]. In the past few years, various Au NCs and Ag NCs have been synthesized by different stabilizers, while the researches on non-noble metal Cu NCs are still limited [4]. Compared with Au and Ag, Cu is extremely cheap, common and of general concern [5]. However, it is apt to oxidize in the air leading to its instability [6]. Therefore, it is necessary to find suitable stabilizers to enhance the stability of clusters. In recent years, proteins have been widely used as templates to synthesize Cu NCs. Protein molecules are rich in sulfhydryl, amino, and carboxyl functional groups, which have a strong ability to coordinate Cu (II) ions and fix the subsequent Cu (0) atoms to the protein skeleton [7]. In addition, due to the presence of sulfhydryl groups, some proteins can act on Cu NCs as templates and reductants [8]. Zhang et.al synthesized silk fibroin protein templated Cu NCs with aggregation induced emission enhance characteristics and constructed a sensitive "turn-on" sensor for $S^{2-}$ [9]. Goswami et.al explored transferrin-templated Cu NCs to load doxorubicin for bioimaging and drug delivery [10].

Egg white is rich in ovalbumin, ovaltransferrin, ovalyoid and lysozyme. It is cheap and easily accessible and non-toxic, thus is an excellent template for the synthesis of Cu NCs. Qian et.al prepared chicken egg white protected Cu NCs with blue emission by one-step method in aqueous solution for reversible pH-sensors [11]. Bhamore et.al developed a one-step green microwave–assisted approach for the synthesis of Cu

✉ Yu He
heyu@hubu.edu.cn

[1] Hubei Collaborative Innovation Center for Advanced Organic Chemical Materials, Ministry-of-Education Key Laboratory for the Synthesis and Application of Organic Functional Molecules, College of Chemistry and Chemical Engineering, Hubei University, Wuhan 430062, China

[2] Hubei Province Key Laboratory of Regional Development and Environment Response, Wuhan 430062, China

NCs with orange emission and used as a fluorescent probe for the sensitive detection of thiram and paraquat in water and food samples [12]. These works have been performed regarding the synthesis and applications of the Cu NCs. However, very few works are available to demonstrate the tuning of emission color of the Cu NCs with $Cu^{2+}$ as the precursor and egg white as the stabilizer.

Determination of ethanol in alcoholic drinks is of importance for quality control in the production process [13–16]. Moreover, herbal medicinal products often contain ethanol at substantial level [17]. Therefore, accurate and rapid determination of ethanol content in liquor is of great significance to control the quality and safety of liquor and maintain the health of consumers [18]. In industrial production processes, the methods of ethanol detection are usually density hydrometer and hydrometer, but both require large sample volume [19]. Among other methods for detecting ethanol such as gas chromatographic methods (GC) [20], high-performance liquid chromatographic method (HPLC) [21] and enzymatic method [22]. However, most of these methods are high cost, time and effort, and difficult to meet the requirement of quick test on site [23]. Fortunately, a few of fluorescence sensors based on nanomaterial for detection of ethanol have emerged. These methods not only improve the simplicity and portability of detection, but also have excellent sensitivity and selectivity. Wen et.al designed a visual and fluorometric-sensor paper containing copper nanoclusters (Cu NCs) and carbon dots (CDs) for the monitoring of atmospheric humidity and ethanol [18]. Zhang et.al prepared $SnS/SnS_2$ nanoparticles by one-step hydrothermal treatment and possessed excellent ethanol sensing property [24]. Wu et.al prepared $Au/NaGdF4$: $Yb^{3+}$, $Er^{3+}$ hybrid fluorescent system for rapid detection of ethanol content in liquor [25]. However, the researches in this field are still rare and much more efforts should be devoted to improve the fluorescence method for determination of ethanol.

In this work, we synthesized four different color emitting Cu NCs using chicken egg white as the stabilizer by changing the reaction conditions including the reducing agent and the pH (scheme 1). All reactions were carried out at room temperature. This is a green, facile and cheap method to explore different color emitting CuNCs by the same precursor and stabilizers. Green emitting Cu NCs (G-Cu NCs) with emission wavelength at 526 nm were synthesized with citric acid as reducing agent. Orange emitting Cu NCs (O-Cu NCs) were prepared with hydroxylamine hydrochloride as reducing agent under alkaline conditions, and the emission wavelength was 600 nm. In addition, hydrazine hydrate was used as the reducing agent to prepare the red emitting Cu NCs (R-Cu NCs) with the emission wavelength of 636 nm. On the basis of this experiment, the pH was adjusted to 11 and yellow emitting Cu NCs (Y-Cu NCs) with emission wavelength of 557 nm were

synthesized. Then, the G-Cu NCs was explored for the detection of ethanol based on aggregation induced emission enhancement (AIEE) effect. Besides, a ratiometric fluorescence probe for ethanol was prepared by integrating G-Cu NCs with silicon nanoparticles (Si NPs). The fluorescence emission of G-Cu NCs at 526 nm showed ethanol dependent fluorescent behavior due to their AIEE effect, while fluorescence emission of Si NPs at 441 nm were used as the reference since the blue fluorescence remains constant with the changes of ethanol content. Therefore, we established both single-emission and double-emission fluorescent probe for fast detection of ethanol in aqueous solution based on egg white protected G-Cu NCs. Moreover, probe has a lower detection limit and a wider detection range. And these two methods were applied to the identification of liquor. The multi-color fluorescence of egg white protected Cu NCs open a new avenue to a lot unforeseen applications in food quality monitoring.
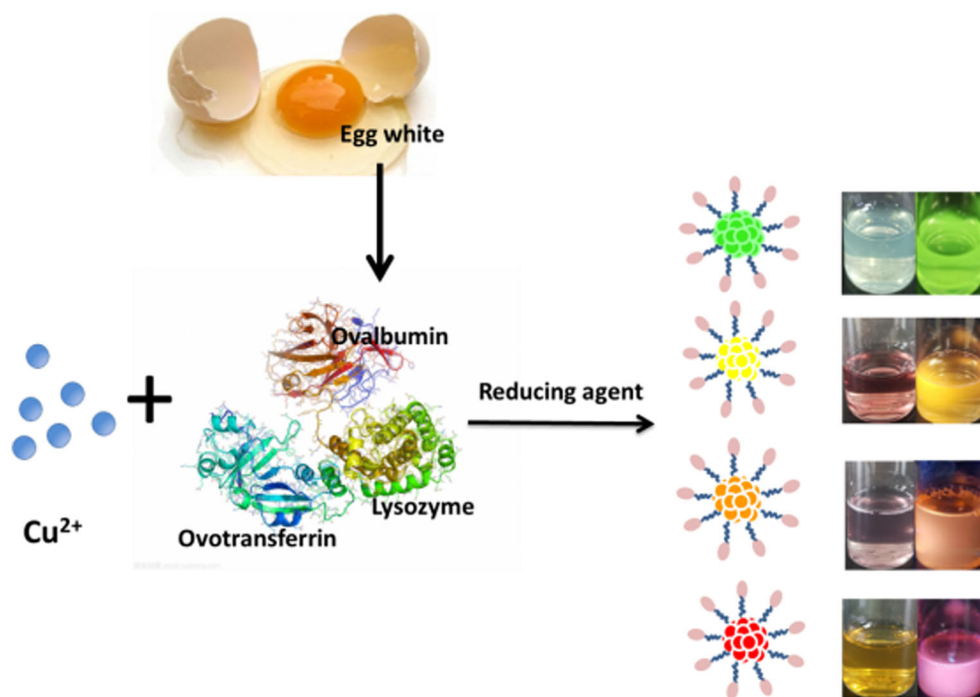
# Experimental

## Chemicals

All reagents were of at least analytical grade. $CuCl_2 \cdot 2H_2O$ was purchased from Macklin Biochemical Co. Ltd. (Shanghai, China). Ascorbic Acid (AA) and (3-Aminopropyl) triethoxysilane (APTES) were ordered from Aladdin Reagent Co. Ltd. (Shanghai, China). Citric acid (CA) was from Tianjin guangcheng chemical reagent Co. Ltd. (Tianjin, China). Ethanol was purchased from Tianjin fuyu fine chemical Co., Ltd. (Tianjin, China). Hydroxylamine chloride was purchased from Tianjin bodi chemical Co., Ltd. (Tianjin, China). Ultrapure water was used throughout all study. All solutions were freshly prepared in deionized water under ambient conditions.

## Apparatus

The fluorescence measurements were carried out on LS55 fluorescence spectrometer (Perkin-Elmer, USA). The UV-vis absorption measurements were performed on Lambda 35 UV analyzer (Perkin-Elmer, USA). High-resolution transmission electron microscopy (HRTEM) was conducted using a JEM-2100 UHR (JEOL, Japan). A Thermo Fisher Escalab 250Xi spectrometer was used for the X-ray photoelectron spectroscopy (XPS) analyses. Fourier Transform Infra-Red (FTIR) spectra were taken with a Spectrum One FTIR spectrophotometer (Perkin-Elmer, USA) at room temperature. The centrifuge was TG 16-II (Pingfan Instrument, China). The homogenizer was AD 200 L-P (Angni Instrument, China).

**Scheme 1** Synthetic scheme of chicken egg white protected Cu NCs



## Synthesis of different color emitting Cu NCs

In experiment, all Cu NCs were synthesized from the same precursor copper chloride and egg whites. The composite diagram is shown in scheme 1. The chicken egg white (CEW) was prepared by separating the white portion of the chicken egg from the whole fresh egg followed by homogenization. The prepared Cu NCs appeared green, yellow, orange and red fluorescence on UV-light irradiation of 365 nm wavelength respectively.

**Synthesis of G-Cu NCs** Briefly, $CuCl_2 \cdot 2H_2O$ (10 mM, 3 mL) and CEW (3 mL) were mixed together for 5 min at room temperature, and citric acid (1 M, 1 mL) was added to react for 2 h under stirring. The obtained solution was purified by centrifugation (9000 r/min, 10 min). Finally, G-Cu NCs was obtained and stored at 4 °C.

**Synthesis of Y-Cu NCs** $CuCl_2 \cdot 2H_2O$ (10 mM, 3 mL) and CEW (3 mL) were mixed together with vigorous stirring for 5 min at room temperature, and 0.25 mL hydrazine hydrate (85%) was added. Then NaOH (1 M) was added until the pH of solution to 11.0 to continuously react for 1 h. Finally, Y-Cu NCs was obtained and stored at 4 °C.

**Synthesis of O-Cu NCs** $CuCl_2 \cdot 2H_2O$ (10 mM, 3 mL) and CEW (3 mL) were mixed together for 5 min at room temperature, and then hydroxylamine hydrochloride (1.5 M, 1.5 mL) was added. The NaOH solution (1 M) was added to adjust the

solution pH of 11.0 to continuously react for 2 h. Finally, O-Cu NCs was obtained and stored at 4 °C.

**Synthesis of R-Cu NCs** $CuCl_2 \cdot 2H_2O$ (10 mM, 3 mL) and CEW (3 mL) were mixed together for 5 min at room temperature, and 0.40 mL hydrazine hydrate (85%) was added to coutinuously react for 6 h. Finally, R-Cu NCs was obtained and stored at 4 °C.

## Synthesis of Si NPs

The Si NPs were synthesized according to the literature [26]. APTES (1.00 mL) was injected into 4.00 mL of aqueous solution in a 40 °C water bath. Then, 1.25 mL of AA (0.1 M) was mixed with the above solution by stirring for 20 min. The resulting Si NPs (124 $mg \cdot mL^{-1}$) were synthesized and stored at ambient temperature for further use.

## Ethanol detection with G-Cu NCs

The different contents of ethanol (5, 10, 15, 20, 25, 30, 35, 40, 45, 50, 55 and 60%) were prepared by adjusting the ratio of ethanol and water. Typically, 25 μL G-Cu NCs were added into 2 mL aqueous solution containing different concentrations of ethanol. These solutions were mixed well and equilibrated for 2 min before fluorescence measurements. Fluorescence emission spectra ($\lambda_{ex}$ = 444 nm) of the sensing system were finally recorded for the quantitative analysis.

## Ethanol detection with SiNPs/G-CuNCs

The assembly of SiNPs and G-CuNCs (SiNPs/G-CuNCs) was fabricated by the following procedure. 2 μL as-obtained SiNPs and 20 μL G-CuNCs were thoroughly mixed to further use. Then various content of ethanol (2, 5, 7, 10, 12, 15, 17, 20%) was added to the sensing system, and fluorescence emission spectra were accordingly recorded with excitation at 383 nm. Smartphone was used to take pictures under a UV lamp at 365 nm.

## Results and discussion

### Characterization of different emitting Cu NCs

The synthesis diagram of different fluorescence emitting Cu NCs protected by egg white is shown in Scheme1. The emission and excitation spectra for G-Cu NCs, Y-Cu NCs, O-Cu NCs and R-Cu NCs are given in Fig. 1. The corresponding fluorescence emission wavelength was 526 nm, 557 nm, 600 nm and 636 nm, respectively. Obvious green, yello.

w, orange and red fluorescence were observed when as-synthesized Cu NCs were illuminated with an UV lamp of 365 nm excitation (inset of Fig. 1). The relative quantum yields (QY) of Cu NCs were measured with different fluorescence dyes as reference. Using quinine sulfate as the reference dye, the QY of Y-Cu NCs, O-Cu NCs and R-Cu NCs were measured to be 0.2%, 0.28% and 2.7% respectively. In addition, the QY of G-Cu NCs was 14.5% with respect to Rhodamine 6G. The QY of G-Cu NCs was much higher than that of Y-Cu NCs, O-Cu NCs and R-Cu NCs. The stability of

the Cu NCs were also investigated in Fig. S2. The fluorescence intensity of four different Cu NCs were keep constant in 24 h, which demonstrated their stability. Based on the excellent optical properties of G-Cu NCs, further application of G-Cu NCs were explored.

XPS measurements were performed to confirm the chemical state and composition of G-Cu NCs, Y-Cu NCs, O-Cu NCs and R-Cu NCs. As shown in Fig. 2a-d, two distinct peaks were observed at 932.6 eV and 952.3 eV were assigned to be the binding energies of 2p3/2 and 2p1/2 electrons of Cu (0) and Cu (I) in all the XPS spectra of four color emitting Cu NCs, respectively. These results indicated that Cu NCs mainly consist of Cu (0) and Cu (I) [27].

TEM spectra of G-Cu NCs, Y-Cu NCs, O-Cu NCs and R-Cu NCs are shown in Fig. 3. The four different color Cu NCs were well-dispersed with spherical shape. The average particle size of G-Cu NCs was 2.8 nm (inset in Fig. 3a). For Y-Cu NCs, O-Cu NCs and R-Cu NCs, the average particle size was 3.4 nm (inset in Fig. 3b), 2.5 nm (inset in Fig. 3c) and 3.7 nm (inset in Fig. 3d) respectively, which demonstrated that the size distributions of Cu NCs were affected by reaction conditions for the same precursors. The FTIR spectra of the pure CEW and the four kinds of Cu NCs were measured and the results were shown in Fig. S1. In curve c of Fig. S1, the characteristic absorption of protein amide I band (1656 $cm^{-1}$) were disappeared in the spectra of O-Cu NCs, which indicated that formation of O-Cu NCs might perturb the conformation of protein molecules in CEW. According to curve b of Fig. S1, compared with the FTIR spectra of CEW the characteristic absorption of O-H or N-H shifted from 3300 $cm^{-1}$ to 3575 $cm^{-1}$, and the stretching vibration of CH at 2959 $cm^{-1}$ shifted to 3015 $cm^{-1}$, indicating that the



**Fig. 1** Fluorescence excitation and emission spectra of (a) G-Cu NCs, (b) Y-Cu NCs, (c) O-Cu NCs and (d) R-Cu NCs. Inset: The digital photo of different color emitting Cu NCs under a UV lamp at 365 nm respectively
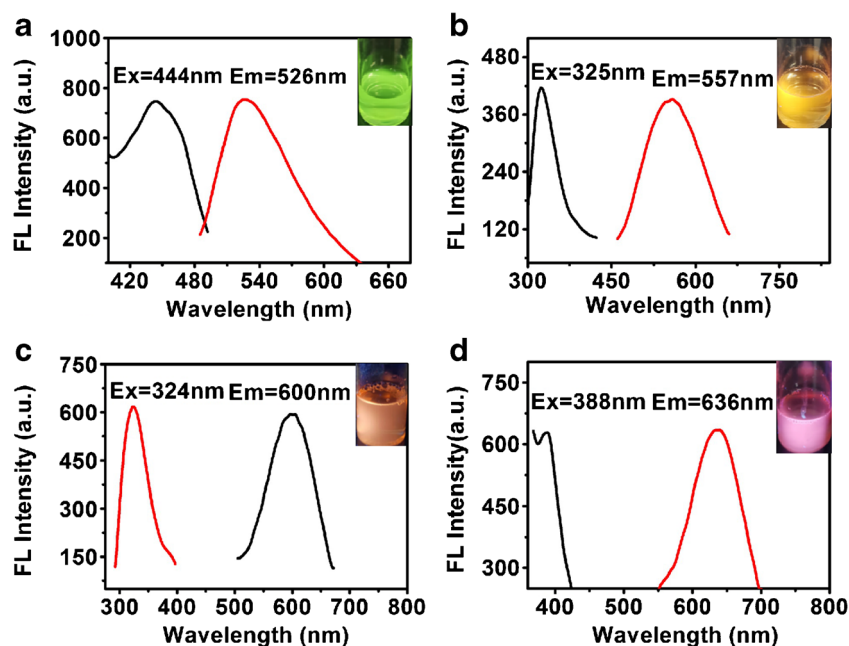
**Fig. 2** XPS spectra of (a) G-Cu
NCs (b) Y-Cu NCs (c) O-Cu NCs
(d) R-Cu NCs Cu NCs
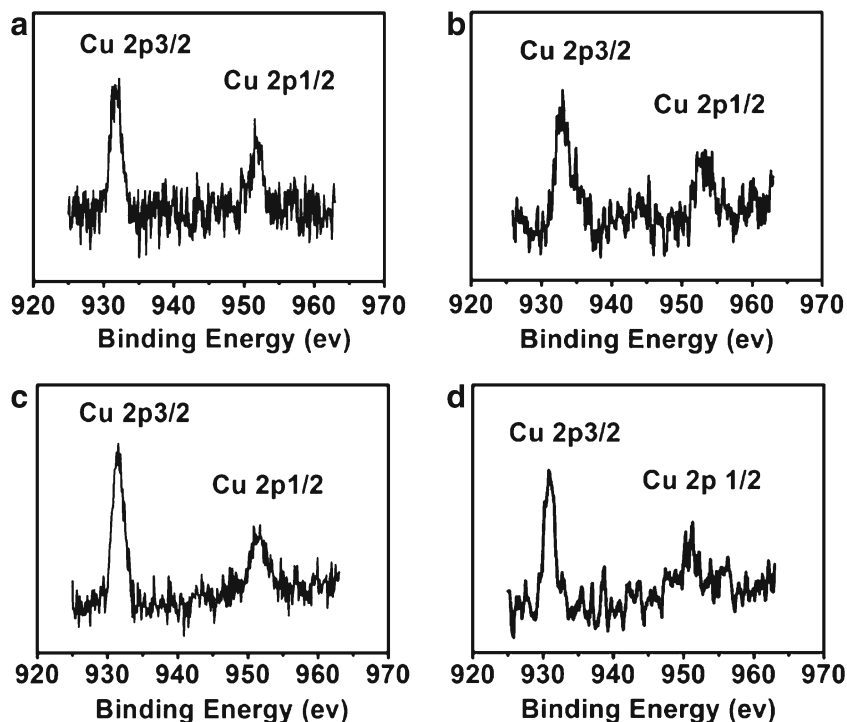


formation of G-Cu NCs. Similarly, in the curve a and d of Fig.
S1, the absorption peak positions of the Y-Cu NCs and R-Cu
NCs at 3300 cm$^{-1}$, 2959 cm$^{-1}$, 1656 cm$^{-1}$ also changed re-
spectively, indicating that the interactions between CEW and
the Cu NCs.

## The fabrication of fluorescence probe for ethanol based on G-Cu NCs

In this study, G-Cu NCs and Si NPs/G-Cu NCs fluorescent
probe was established for the quantitative sensing of ethanol.

**Fig. 3** TEM image of (a) G-
CuNCs; (b) Y-CuNCs; (c) O-
CuNCs; (d) R-CuNCs. Inset: the
size distribution for four kinds of
Cu NCs
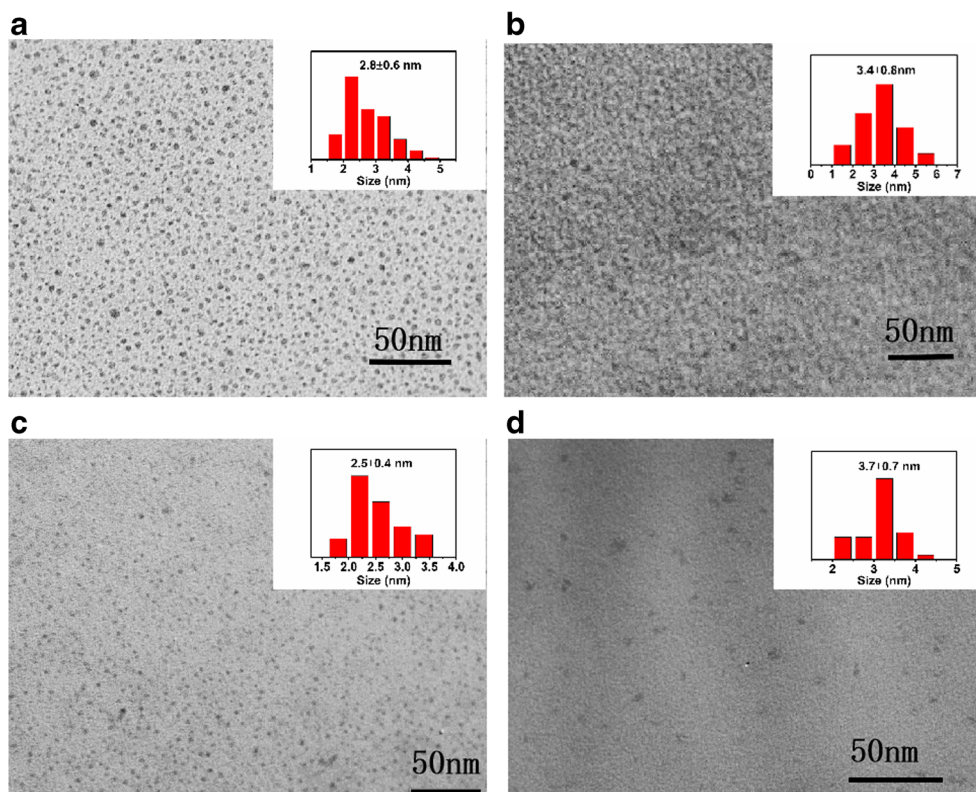
**Table 1** The comparison of the method of the report and the measurement method of the present determination of ethanol content

| Materials | Methods | Analytical range (%) | Detection limit (%) | References |
|---|---|---|---|---|
| biNAP | Fluorescence | 40–70 | | [31] |
| CDs-CuNCs | Fluorescence | 20–60 | | [18] |
| GSH-CuNCs | Fluorescence | 0–50 | | [32] |
| | | 65–80 | | |
| Au/NaGdF$_4$:Yb$^{3+}$,Er$^{3+}$ hybrid | Fluorescence | 25–90 | | [25] |
| G-Cu NCs | Fluorescence | 5–60 | 0.17 | This work |
| Si NPs/G-Cu NCs | Fluorescence | 2–20 | 0.06 | This work |

The prepared G-Cu NCs showed strong green photoluminescence under UV light, and emission peaks at 526 nm were recorded at the optimum excitation wavelength of 444 nm as shown in Fig. S3a. The G-Cu NCs have strong green fluorescence with the quantum yield of 14.5% and excellent fluorescence stability (Fig. S4). The HRTEM image of shown in set of Fig. S3b displayed the highly crystalline structure of the G-Cu NCs with the lattice fringe spacing of 0.315 nm. The Si NPs were characterized by fluorescence, TEM and XPS spectroscopy respectively. In Fig. S3c, under excitation at 383 nm, the maximum emission of Si NPs was centered at 447 nm. The aqueous solution of Si NPs exhibited blue fluorescence under UV light at 365 nm (inset in Fig. S3c). TEM image in Fig. S3d displayed that Si NPs were dispersed well with the average particle size of 2.0 nm. The full range XPS analysis (Fig. S5) of Si NPs clearly showed five peaks at 101.74, 284.11, 398.24, and 531.02 eV corresponding to the elements of Si 2p, C 1 s, N 1 s, and O 1 s, respectively [28, 29]. After simply blending Si NPs and G-Cu

NCs, the ratiometric fluorescent performance was mainly based on the fluorescence resonance energy transfer (FRET) between Si NPs and G-Cu NCs. Emission spectra of Si NPs/G-Cu NCs presented two peaks at around 441 nm and 525 nm under the excitation wavelength of 383 nm (Fig. S3e), corresponding to the blue and green fluorescence of Si NPs and G-CuNCs respectively. The TEM image showed clearly that the Si NPs and G-CuNCs were able to assemble into well-defined spherical particles with diameter about 62.8 nm (Fig. S3f).

The effects of different ethanol contents on G-CuNCs were studied in Fig. 4a. With the increase of the contents of ethanol varying from 0 to 60%, the fluorescence of CuNCs at 526 nm gradually increased under the excitation of 444 nm. The mechanism for response was based on the AIEE effect of G-CuNCs [30]. As shown in Fig. 4b, the value of $(F-F_0)/F_0$ have a linear relationship with the contents of ethanol in the range from 5 to 25% (Fig. 4c) and 25–60% (Fig. 4d), the regression equation can be described as: $(F-F_0)/F_0 = 0.03293$ V%-0.12863 ($R^2 = 0.9798$), $(F-F_0)/F_0 = 0.01028$ V% + 0.45663

**Fig. 4** (a) Fluorescence spectra of sensing system in the various ethanol contents from 0 to 60% ($\lambda_{ex} = 444$ nm); (b) scatter diagram and the fitting curve between fluorescence enhancement efficiency and ethanol contents in the range from 5 to 25% (c) and 25 to 60% (d)
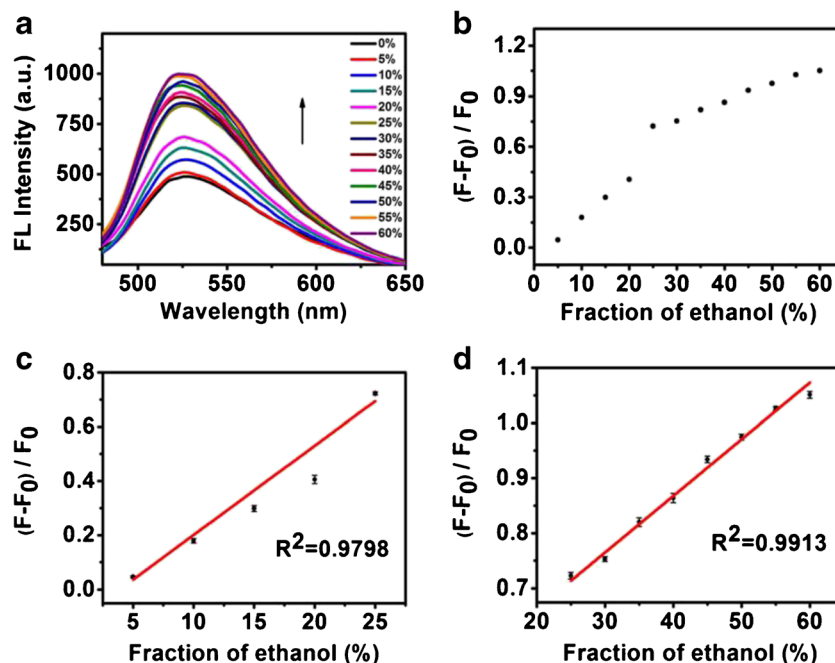
**Fig. 5** (a) Fluorescence spectra of Si NPs/G-Cu NCs in different concentrations of ethanol from 0% to 20% ($\lambda_{ex} = 383$ nm). (b) The linear relationship between the ratio of fluorescence intensity ($I_{525}/I_{441}$) and ethanol contents between 2 to 20%. (c) The digital photo of SiNPs/G-CuNCs in solutions containing different ethanol contents under 365 nm UV light
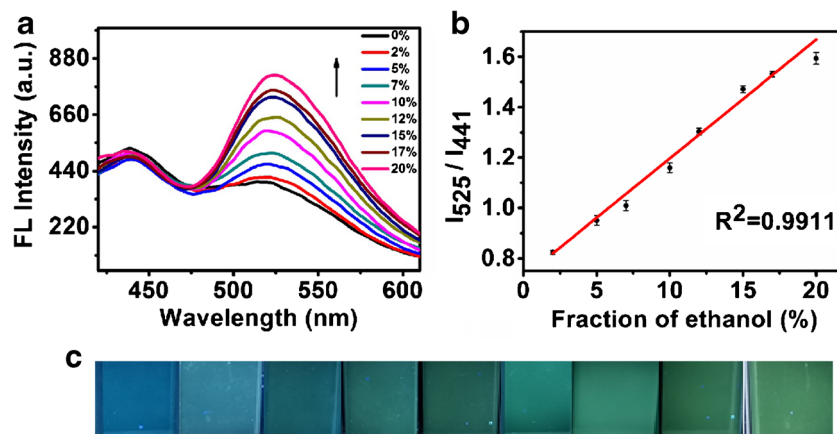
($R^2 = 0.9913$), V% refers to the contents of ethanol. The limit of detection is 1.67% according to LOD = 3 /s, where is the standard deviation of the blank and s is the slope of the calibration plot. Compared with other methods probe for ethanol detection, this probe showed a lower detection limit and a wider detection range (Table 1).

Inspired by the solvent-dependent effect of G-CuNCs, we also designed a ratio fluorescence probe based on Si NPs as a reference to detect ethanol. As shown in Fig. 5a, under the excitation of 383 nm, with the increase of ethanol content, the CuNCs fluorescence at 525 nm increased whereas the SiNPs fluorescence at 441 nm remained almost constant. By plotting the $I_{525}/I_{441}$ values against ethanol content, a good linear relationship can be obtained in the range of 2–20% (Fig. 5b). The regression equation can be described as: $I_{525}/I_{441} = 0.04714$ V% $+ 0.7254$ ($R^2 = 0.9911$), with the limit of detection of 0.06%. The comparison between previous reported methods and our methods was displayed in Table 1. Our single-emission fluorescent probe and the double-emission fluorescent probe for ethanol have lower detection limits of 0.17% and 0.06%, respectively. Especially for double-emission fluorescent probe, this ratiometric fluorescent sensor is consisted of G-Cu NCs as the indicator signal and Si NPs as a reference signal to construct a stable detection system

through self-calibration, which avoid some errors induced by interference. Additionally, the color change of dual emission fluorescent probe is obvious and easily distinguished by the naked eye under a UV lamp which can facilitate the on-site, real-time, and portable measurement. The SiNPs/G-CuNCs system exhibited an obvious fluorescence color change from blue to green under a UV lamp with increased concentration of ethanol (Fig. 5c), implying the potential of SiNPs/G-CuNCs for the semiquantitative analysis of ethanol.

## Selectivity for the detection of ethanol

We investigated selectivity for the detection of ethanol by our method. The G-CuNCs or Si NPs/G-Cu NCs system gave excellent selectivity for detecting ethanol in the presence of main interference in the actual sample liquor such as methanol, acetic acid, ethylene glycol and ethyl acetate (Fig. 6a and Fig. 6b). When the concentration of ethanol was 10 times than that of interference, the interference had little effect on the single emission and double emission ethanol sensing system. The results demonstrated that G-Cu NCs and Si NPs/G-Cu NCs sensing systems have good selectivity for the detection of ethanol in liquor samples.

**Fig. 6** (a) Fluorescence response of (a) G-CuNCs and (b) Si NPs/G-Cu NCs to 20% ethanol and 2% methanol, acetic acid, ethylene glycol and ethyl acetate respectively
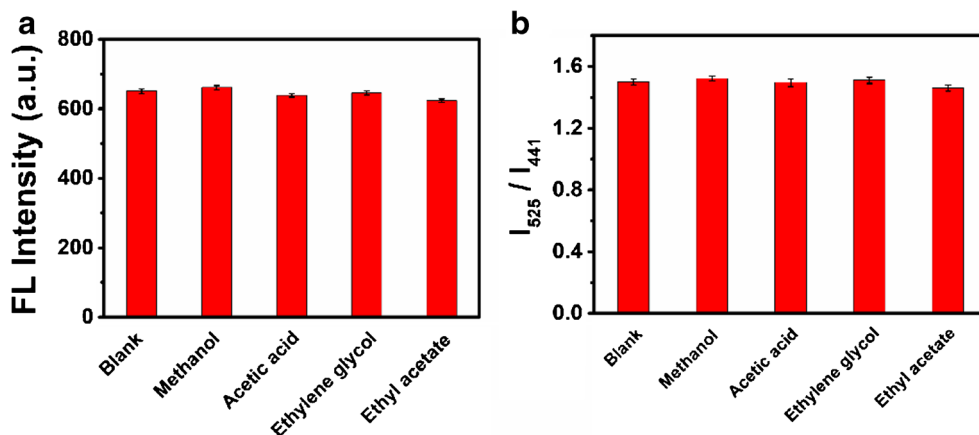
## Detection of ethanol content in real samples

For the real samples testing, we used 40, 50 and 56 degree liquor purchased from local supermarket to evaluate the ethanol content by G-CuNCs and Si NPs/G-Cu NCs system. For the SiNPs/G-CuNCs system, an appropriate (4-fold) dilution of liquor was found sufficient to obtain a quantitative recovery (93.2–113%) of spiked ethanol and to use a simple aqueous standard solution for the accurate quantification of ethanol with RSD in the range of 0.45%–1.25% (Table S1 and Table S2).

## Conclusion

A cost-effective and straightforward chicken egg white directed synthesis approach was applied to prepare Cu NCs with green, yellow, orange and red emission. The G-Cu NCs was applied for the detection of ethanol due to their AIEE effect. We also designed a double-emission probe for ethanol exploring Si NPs serve as the fluorescence reference. In addition, fluorescent color changes of the ratio sensor (Si NPs/G-Cu NCs) from blue to green could be observed, which is beneficial for semi-quantitative analysis. For the actual sample, liquor of 40, 50 and 56 degrees were tested, respectively. The recoveries in liquor were in the range of 99.7% to 113%. The ethanol sensing platforms were applied to the detection and evaluation of the alcohol content of liquor, broadening the applications of Cu NCs and providing a sensitive detection method for ethanol.

## Declarations

**Conflict of interest** The authors declare that they have no conflict of interest.

## References

1. Liu G, Feng D, Hua D, Liu T, Qi G, Wang W (2017) Fluorescence enhancement of terminal amine assembled on gold Nanoclusters and its application to Ratiometric lysine detection. Langmuir 33(51):14643–14648. https://doi.org/10.1021/acs.langmuir.7b02614
2. Xie Y, Shen Y, Duan G et al (2020) Silver nanoclusters: controlled synthesis, structures and photoluminescence. Materials Chemistry Frontiers 4(8):2205–2222. https://doi.org/10.1039/D0QM00117A
3. Wu Z, Liu J, Gao Y, Liu H, Li T, Zou H, Wang Z (2015) Assembly-induced enhancement of cu Nanoclusters luminescence with Mechanochromic property. J Am Chem Soc 137(40):12906–12913. https://doi.org/10.1021/jacs.5b06550
4. Darugar Q, Qian W, El-Sayed MA, Pileni MP (2005) Size-dependent ultrafast electronic energy relaxation and enhanced fluorescence of copper nanoparticles. J Phys Chem B 110:143–149. https://doi.org/10.1021/jp0545445
5. Lin L, Hu Y, Zhang L, Huang Y, Zhao S (2017) Photoluminescence light-up detection of zinc ion and imaging in living cells based on the aggregation induced emission enhancement of glutathione-capped copper nanoclusters. Biosens Bioelectron 94:523–529. https://doi.org/10.1016/j.bios.2017.03.038
6. Biswas S, Miller JT, Li Y, Nandakumar K, Kumar CSSR (2012) Developing a millifluidic platform for the synthesis of ultrasmall nanoclusters: ultrasmall copper nanoclusters as a case study. Small 8:688–698. https://doi.org/10.1002/smll.201102100
7. Qing T, Zhang K, Qing Z, Wang X, Long C, Zhang P, Hu H, Feng B (2019) Recent progress in copper nanocluster-based fluorescent probing: a review. Microchim Acta 186(10):670–689. https://doi.org/10.1007/s00604-019-3747-4
8. Xu Y, Sherwood J, Qin Y, Crowley D, Bonizzoni M, Bao Y (2014) The role of protein characteristics in the formation and fluorescence of au nanoclusters. Nanoscale 6:1515–1524. https://doi.org/10.1039/c3nr06040c
9. Zhang G, Wang R, Shi L, Zhang C, Zhang Y, Zhou Y (2019) Aggregation/assembly induced emission based on silk fibroin-templated fluorescent copper nanoclusters for "turn-on" detection of $S^{2-}$. Sensors Actuators B Chem 279:361–368. https://doi.org/10.1016/j.snb.2018.09.100
10. Goswami U, Dutta A, Raza A (2018) Transferrin-copper Nanocluster-doxorubicin nanoparticles as targeted Theranostic Cancer Nanodrug. ACS Appl Mater Interfaces 10(4):3282–3294. https://doi.org/10.1021/acsami.7b15165
11. Qian Y, Xu T, Zhang Y et al (2015) Green synthesis of fluorescent copper nanoclusters for reversible pH-sensors. Sensors Actuators B Chem 220:1064–1069. https://doi.org/10.1016/j.snb.2015.06.073
12. Bhamore JR, Jha S, Mungara AK (2016) One-step green synthetic approach for the preparation of multicolor emitting copper nanoclusters and their applications in chemical species sensing and bioimaging. Biosens Bioelectron 80:243–248. https://doi.org/10.1016/j.bios.2016.01.066
13. Jung H, Verwilst P, Kim W, Kim J (2016) Fluorescent and colorimetric sensors for the detection of humidity or water content. Chem Soc Rev 45:1242–1256. https://doi.org/10.1039/c5cs00494b
14. Hernaez M, Mayes AG, Melendi-Espina S (2017) Graphene oxide in lossy mode resonance-based optical fiber sensors for ethanol detection. Sensors 18:58. https://doi.org/10.3390/s18010058
15. Zhang C, Lin N, Chai X, Zhong L, Barnes D (2015) A rapid method for simultaneously determining ethanol and methanol content in wines by full evaporation headspace gas chromatography. Food Chem 183:169–172. https://doi.org/10.1016/j.foodchem.2015.03.048
16. Zhang L, Qi H, Wang Y, Yang L, Yu P, Mao L (2014) Effective visualization assay for alcohol content sensing and methanol differentiation with solvent stimuli-responsive supramolecular ionic materials. Anal Chem 86:7280–7285. https://doi.org/10.1021/ac5014546
17. Kelber O, Steinhoff B, Nauert C, Biller A, Adler M, Abdel-Aziz H, Okpanyi SN, Kraft K, Nieber K (2017) Ethanol in herbal medicinal products for children. Wien Med Wochenschr 167(7–8):183–188. https://doi.org/10.1007/s10354-016-0474-x
18. Wen Z, Song S, Wang C, Qu F (2019) Large-scale synthesis of dual-emitting-based visualization sensing paper for humidity and ethanol detection. Sensors Actuators B Chem 282:9–15. https://doi.org/10.1016/j.snb.2018.11.041

19. Thungon P, Kakoti A, Ngashangva L, Goswami P (2017) Advances in developing rapid, reliable and portable detection systems for alcohol. Biosens Bioelectron 97:83–99. https://doi.org/10.1016/j.bios.2017.05.041

20. Li H, Chai X, Deng Y, Zhan H, Fu S (2009) Rapid determination of ethanol in fermentation liquor by full evaporation headspace gas chromatography. J Chromatogr A 1216(1):169–172. https://doi.org/10.1016/j.chroma.2008.11.024

21. Tagliaro F, Dorizzi R, Ghielmi S, Marigo M (1991) Direct injection high-performance liquid chromatographic method with electrochemical detection for the determination of ethanol and methanol in plasma using an alcohol oxidase reactor. J Chromatogr B Biomed Sci Appl 566(2):333–339. https://doi.org/10.1016/0378-4347(91)80249-C

22. Wang, S, Yan, H, Wang, Y, Wang, N (2019) Hollow Prussian Blue nanocubes as peroxidase mimetic and enzyme carriers for colorimetric determination of ethanol. Microchimica Acta186(11):738–745. https://doi.org/10.1007/s00604-019-3826-6

23. Li B, Wang W, Xu S, Xu S, Chen X, Chen X (2018) 无酶光电化学法快速检测酒类中的乙醇含量 Chinese J. anal. Chem 46(8):1208–1214

24. Zhang Q, Ma S, Zhang R, Tie Y et al (2020) Optimization ethanol detection performance manifested by SnS /SnS$_2$ nanoparticles. Mater Lett 258:126783. https://doi.org/10.1016/j.matlet.2019.126783

25. Wu S, Wu X, Nie G et al (2019) Au/NaGdF$_4$: Yb$^{3+}$, Er$^{3+}$ hybrid fluorescent system for rapid detection of ethanol. Mater. Res. Bull (109):55-159. https://doi.org/10.1016/j.materresbull.2018.09.036

26. Ma S, Chen Y, Feng J, Liu J, Zuo X, Chen X (2016) One-step synthesis of water-dispersible and biocompatible silicon nanoparticles for selective heparin sensing and cell imaging. Anal Chem 88:10474–10481. https://doi.org/10.1021/acs.analchem.6b02448

27. Huang Y, Feng H, Liu W, Zhou Y, Tang C (2016) Luminescent aggregated copper Nanoclusters Nanoswitch controlled by hydrophobic interaction for real-time monitoring of acid phosphatase activity. Anal Chem 88(23):11575–11583. https://doi.org/10.1021/acs.analchem.6b02957

28. Romero JJ, Wegmann M, Rodríguez HB, Lillo C, Rubert A (2015) Impact of Iron incorporation on 2-4 nm size silicon nanoparticles properties. J Phys Chem C 119:5739–5746. https://doi.org/10.1021/acs.jpcc.5b00172

29. Lillo CR, Romero JJ, Portoles ML, Diez RP et al (2015) Organic coating of 1-2-nm-size silicon nanoparticles: effect on particle properties. Nano Res 8(6):2047–2062. https://doi.org/10.1007/s12274-015-0716-z

30. Jia X, Li J, Wang E (2013) Cu Nanoclusters with aggregation induced emission enhancement. Small 9(22):3873–3879. https://doi.org/10.1002/smll.201300896

31. Zhang Y, Qu Y, Zhu Y, Wu J, Rui Y (2019) Bisnaphthalimide-based fluorescent sensor for detecting alcohol and application in evaluating the liquors. J Lumin 214:116573. https://doi.org/10.1016/j.jlumin.2019.116573

32. Guo X, Zhou Y, Shi L, Zhang Y (2018) Luminescence emission of copper Nanoclusters by ethanol-induced aggregation and aluminum ion-induced aggregation. Acta Phys -Chim Sin 34(7):818–824. https://doi.org/10.3866/PKU.WHXB201712081